Geochemistry of some Ferrar Large Igneous Province intrusive rocks in the Transantarctic Mountains, Antarctica

A Senior Thesis

Submitted in partial fulfillment of the requirements for the

Bachelor of Science Degree

At The Ohio State University

by

Megan Harris

The Ohio State University

2014

Approved by

David H Elliot

Dr. David H Elliot, Advisor
School of Earth Sciences

Table of Contents

Acknowledgements

I am overwhelmed with gratitude to Dr. David H Elliot for his patience and guidance as my thesis advisor. This paper would not have been possible without his support, time, and instruction.

I would like to acknowledge the Byrd Polar Rock Repository and its NSF Funding for providing the samples that I analyzed.

I would like to thank Anthony Lutton (ICP-MS and ICP-OES Lab), Steven Goldsmith and Kelly Deuerling (XRF Lab), and Julie Codispoti (Byrd Polar Rock Repository). You all gave me your time, and allowed me the opportunity to utilize your labs and necessary equipment in order to analyze my samples.

This research project would not have been possible without the funding provided by Shell Exploration and Production Company, The Ohio State University College of Arts and Sciences Undergraduate Research Scholarship, and the National Science Foundation grant ANT 0739720.

I would like to thank my family for always believing in me, no matter what.

I would finally like to thank my Mom and my son. You two have inspired me to come back and finish this part of my life. Without your inspiration I would be lost.

List of Figures and Tables

Abstract

The Ferrar Large Igneous Province is a widespread magmatic event associated with the break-up of Gondwana during the Jurassic Period. The Ferrar outcrops over a distance of 3000 km throughout the Transantarctic Mountains. It consists of the Ferrar Dolerites, the Dufek intrusion, Kirkpatrick basalts and pyroclastic rocks. Twenty samples collected from Ferrar sills within the Beardmore Glacier region and elsewhere were analyzed to determine the presence of additional olivine-bearing sills and the continuity of the Mount Fazio Chemical Type (MFCT) composition throughout the region. All samples analyzed have been determined to be of the MFCT composition, including a set of samples that are olivine-bearing, and a single sample that belongs to the Dufek intrusion rather than the Ferrar Dolerite. The research expands the geochemical data base and stratigraphic coverage of the Ferrar Large Igneous Province.

I. Introduction

The Ferrar Large Igneous Province, a large-scale magmatic emplacement of Jurassic age, crops out in the Transantarctic Mountains, the mountain range that divides West Antarctica from East Antarctica (Elliot and Fleming, 2008). The Transantarctic Mountains span a length of over 3000 km (Fig. 1). The Ferrar Large Igneous Province is found throughout the length of the snow and ice-covered Transantarctic Mountains, with rock outcrops that can be traced continually for several tens of kilometers (Elliot and Fleming, 2008). The Ferrar Large Igneous Province comprises mainly intrusive rocks, known as Ferrar Dolerites, and extrusive lava flows, known as the Kirkpatrick Basalt (Fleming et al., 1997). The Ferrar Dolerite occurs primarily as sills, large horizontal sheets emplaced into older sedimentary rock sequences, and dikes which were vertical conduits. At a few localities the sills may be as thick as 700 m, but primarily range 100-300 m thick (Elliot and Fleming, 2004). Although the Ferrar Large Igneous Province is identified throughout the entire Transantarctic Mountains, the largest exposures of sills are found in the Shackleton and Beardmore Glacier regions (Elliot and Fleming, 2004). In these regions the exposed sills intrude the Devonian to Triassic sedimentary sequence known as the Beacon Supergroup (Elliot and Fleming, 2004). An identifiable characteristic of Large Igneous Provinces is that they not only cover an extremely large area and have great volume (> 2 million km^3), but are estimated to have been emplaced over a relatively short period of time (≤ 1 million years) which implies a high rate of magmatism (Heimann et al., 1994).

As of now, the best estimate radiometric age for the Ferrar province is 183.6 ± 1.8 Ma (Elliot and Fleming, 2008), with an estimated duration of emplacement of ≤ 1 million years (Heimann et al., 1994). Geochemical analysis of the Ferrar Large Igneous Province has

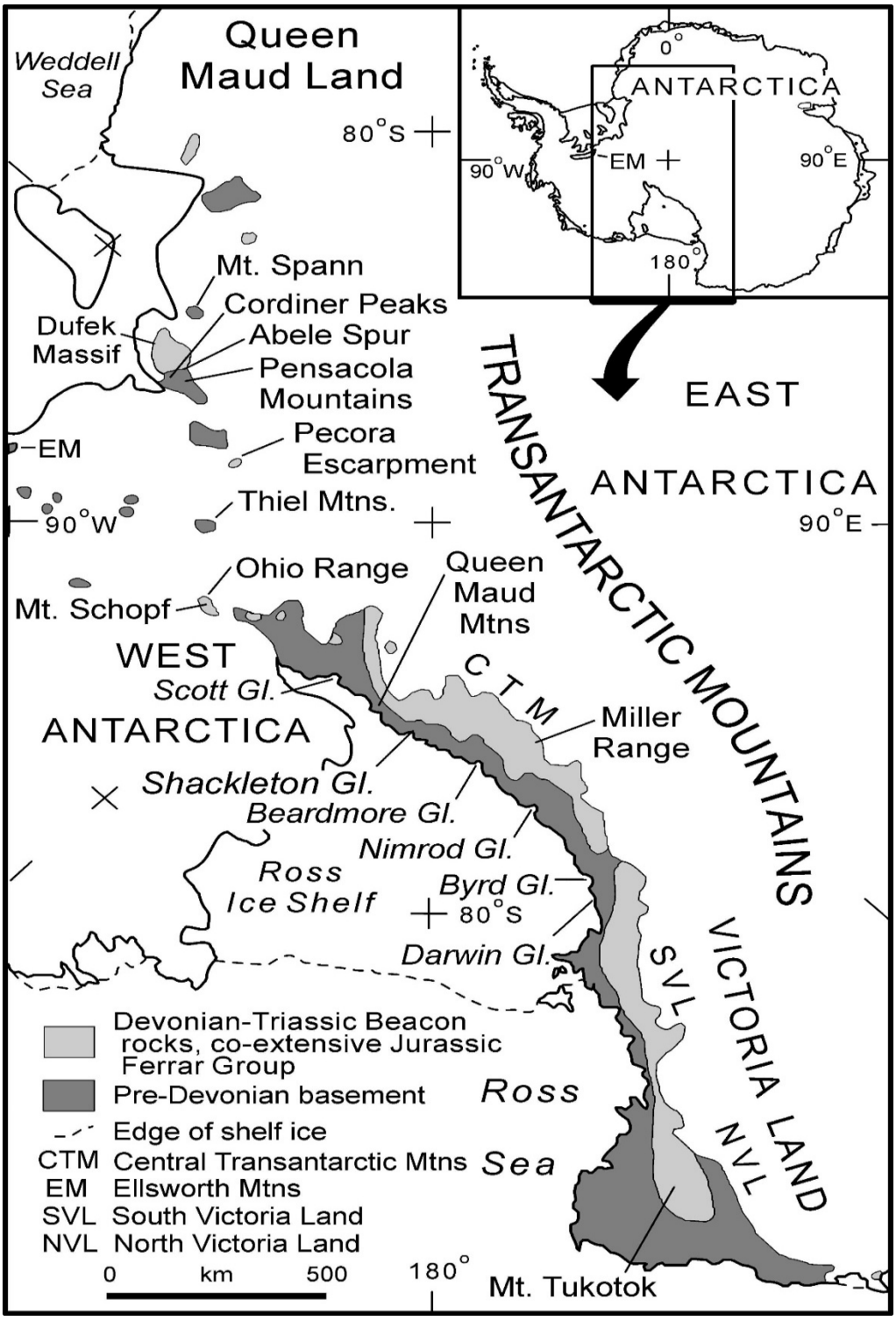

Fig.1. Map of Antarctica showing distribution of the Beacon Supergroup, Ferrar Group, other Jurassic Tholeiites, and undifferentiated bedrock

determined that there are two main chemical types, the Scarab Peak Chemical Type (SPCT) and the Mount Fazio Chemical Type (MFCT) (Fleming et al., 1997). Geochemically, the SPCT is a more highly evolved composition (MgO=2.3%) that has been identified in the uppermost lava flows of the Ferrar Large Igneous Province and in sills in the Whichaway Nunataks, and Theron Mountains. Approximately 99% of the Ferrar Large Igneous Province belongs to the MFCT (Fleming et al., 1997; Elliot et al., 1999). Based principally on lava flows, the MFCT is subdivided into three groups of geochemical compositions (MgO=3-4%, MgO=6-7.5%, MgO=9%). The chemical range and isotopic variations, from mafic to more silicic, are evidence of magma evolution by the processes of fractional crystallization and crustal assimilation (Fleming et al., 1995). The evolved but coherent SPCT chemical and isotopic compositions suggest the Ferrar province has a single point source (Fleming et al., 1997; Elliot et al., 1999).

The accurate and precise dating of the emplacement of the Ferrar Dolerites is an issue that is currently being investigated by other researchers. Until very recently radiometric dating methods, although relatively accurate, have had an uncertainty that is greater than the estimated duration of emplacement. High precision dating techniques on zircon crystals are being used in order to reduce the uncertainties by one order of magnitude in dates obtained (Burgess et al. 2011). With increased accuracy and precision of dating and a consistent continuum of geochemical variations it is anticipated that the space-time-geochemical relationship of the Ferrar rocks may be elucidated for the Shackleton and Beardmore Glacier regions. If this relationship for the Ferrar Large Igneous Province can be traced through the entire length of the Transantarctic Mountains, correlation of space-time-geochemistry will be of great importance for the explanation of the geologic processes involved in the formation of this and other Large Igneous Provinces.

II. Regional Geology of Central Transantarctic Mountains

The pre-Devonian basement is characterized by granite batholiths intruded into metavolcanic and metasedimentary rocks, and affected by two separate tectonic events (Stump, 1991). These two events were the Beardmore Orogeny, which occurred in the Late Proterozoic, and the Ross Orogeny, which occurred during the Cambrian and early Ordovician.

Nimrod Group, Beardmore Group and Byrd Group - Precambrian to Ordovician

The oldest known rocks of the Central Transarctic Mountains (CTM) are the basement amphibolite-grade metamorphic rocks identified as the Nimrod Group (Stump, 1995; Collinson et al., 1994). These rocks, with protoliths as old as Archean, were deformed and metamorphosed in the mid-Proterozoic (1.7Ga; Goodge and Fanning, 2002). The Nimrod Group is succeeded by, but is not in contact with, the Beardmore Group, which comprises metasedimentary graywacke and shale (Stump, 1995). The folding and metamorphism of the Beardmore Group is referred to as the Beardmore Orogeny, and dated as Late Proterozoic to Early Cambrian (Collinson et al., 1994). The age of the Beardmore Group is uncertain but was deposited prior to the Early Cambrian, which is the oldest age of the overlying Byrd Group (Stump, 1995; Collinson et al., 1994). The upper contact of the Beardmore Group is an angular unconformity on which the Lower Cambrian to Ordovician Shackleton Limestone of the Byrd Group was deposited (Stump, 1995).

The Shackleton Limestone has been measured to be between 1000 and 2000m thick, with an overall apparent thickness up to 5400m due to tectonic stacking (Collinson et al., 1994). The Shackleton Limestone contains many small shelly fossils that are of Early-Middle Cambrian age. The Shackleton Limestone is overlain by the Douglas Conglomerate. These two formations have

undergone at least three episodes of deformation (Collinson et al., 1994; Stump, 1995). The Granite Harbour Intrusives were emplaced in the Nimrod, Beardmore, and Byrd groups during the Ross Orogeny (Collinson et al., 1994), as a result of subduction at the continental margin of East Antarctica.

Beacon Supergroup

The Beacon Supergroup of the Transantarctic Mountains spans the Devonian to the Jurassic. It is a relatively flat-lying sequence up to 2.5 km thick, and is traceable laterally for almost 3000 km (Barrett, 1991; Collinson et al., 1994). The Beacon Supergroup has been interpreted to have been deposited in a foreland basin, the result of compressive tectonics at a convergent margin (Collinson et al., 1994). The sequences that comprose the Beacon Supergroup record various fluvial and glacial environments, and are capped by the basaltic rocks of the Jurassic Ferrar Group.

Taylor Group – Devonian

The deposition of the Beacon Supergroup began during the Devonian with the Taylor Group. The uppermost surface of the Byrd Group is an easily identifiable unconformity, and is referred to as the Kukri Erosion Surface on which the Taylor Group was deposited (Barrett, 1991; Isbell, 1999). The basal unit of the Beacon Supergroup, the Alexandra Formation, is a quartzose sandstone that has a maximum thickness of 300 m (Barrett, 1991; Collinson et al., 1994). There are no shelly fossils in the Alexandra Formation to determine age, but trace fossils and paleocurrent analysis show evidence of deposition in a shallow coastal environment (Collinson et al., 1994).

Victoria Group – Carboniferous - Permian

The upper surface of the Alexandra Formation is a heavily eroded surface known as the Maya Erosion Surface. This disconformity marks the top of the Taylor Group and the base of the Victoria Group (Barrett, 1991). The Pagoda Tillite, the oldest formation of the Victoria Group, is a diamictite of glacial origin. Pollen and spores allow the age of the Pagoda to be determined as late Carboniferous (Collinson et al., 1994). The glacially deposited diamictite of the Pagoda Formation is interbedded with sandstone and mudstone, and is 100 – 200 m thick (Barrett, 1991; Collinson et al., 1994). Clasts in the Pagoda are granite and quartzite which were derived from basement rocks and the Alexandra Formation (Barrett, 1991). Cyclic sequences of glacial advance and retreat are recorded in the diamictites (Collinson et al., 1994). The diamictite was deposited by a terrestrial ice sheet, and the ice sheet's movement can be tracked using glacial striae. The paleoflow was consistently parallel to the present-day Transantarctic Mountains, and toward the southeast (Barrett, 1991; Collinson et al., 1994). This interpretation of the ice flow direction is further supported by the increasing thickness of glacial strata in the same southeast direction (Barrett, 1991).

The Pagoda Tillite is overlain by a regressive sequence of post-glacial shale and fine sandstones, known as the Mackellar Formation. The Mackellar Formation can be subdivided into three major coarsening upwards cycles of interbedded shale and fine-grained sandstone that range in thickness 100 – 200m (Barrett, 1991; Collinson et al., 1994). The first cycle is a fining upward sequence of sandstone beds, and is interpreted as turbidites (Collinson et al., 1994). The second cycle is a series of thick coarsening-up shale with fining-upward channel fill that is capped with thin fining-up sandstones (Collinson et al., 1994). The coarsening-up sequences are evidence of prograding subaqueous deltas (Collinson et al., 1994). High ratios of carbon to

sulfur in the Mackellar shales and low biodiversity preserved suggest the Mackellar Formation was deposited in a freshwater or brackish aqueous environment formed in a crustal depression caused by the former glacial ice cover (Barrett, 1991; Collinson et al., 1994). The paleoflow of the Mackellar Formation was also in a southeastern direction.

The Fairchild Formation is the next stratigraphic formation in the Victoria Group (Barrett, 1991). The Fairchild is an alluvial plain deposit that consists of medium-coarse grained trough cross-bedded sandstones, fine grained ripple and laminated sandstones and shale (Barrett, 1991; Collinson et al., 1994). The Fairchild varies in thickness 130 to 230 m (Collinson et al., 1994). The sandstones are present as interconnected channel-form sheets that range from 5-20 m thick and 10's – 100's m wide (Collinson et al., 1994). The post-glacial sandstones of the Fairchild Formation thins in the northwestern direction, indicating a basin in the Beardmore Glacier region during the time of deposition (Collinson et al., 1994). The Fairchild strata were deposited in an interior sea in which the Mackellar had accumulated by progradation of subaqueous deltaic fans followed by a braided fluvial system (Collinson et al., 1994). The paleocurrent direction of the Fairchild Formation, like the Mackellar Formation, runs southeast parallel to the Transantarctic Mountains.

The Fairchild Formation is overlain by the Buckley Formation. The Buckley Formation extending over 800 km along the CTM, consists of cyclic sequences of sandstone, carbonaceous siltstone and mudstone, and coal (Collinson et al., 1994). The basal unit of a cyclic sequence is 20-30 m thick fining upward, scour-based, medium to coarse, trough cross-bedded channel-form sandstone (Barrett, 1991). Ripple and horizontally-laminated fine-grained siltstone and carbonaceous mudstone drapes were deposited over the underlying sandstones (Collinson et al., 1994). The finer grained beds overlying the channel fill may include coal, which is up to 10m

thick (Barrett, 1991). The depositional environments transitioned from braided streams to large relatively straight channels to a major delta system (Barrett, 1991; Collinson et al., 1994). *Glossopteris* leaves found in abundance in the carbonaceous beds suggest a late Permian age (Collinson et al., 1994). The appearance of *Glossopteris* suggests that the climate in the Beardmore Glacier region changed from cold to cool, which allowed for migration of flora into the environment (Barrett, 1991). The Buckley Formation shows evidence of extensive flood plains, rapid subsidence, and large scale channel migration (Collinson et al., 1994). The low rate of sedimentation from the flood plains and the high rate of subsidence created an underfilled basin in the Beardmore Glacier Region in the Late Permian and Early Triassic (Collinson et al., 1994). A major paleogeographic change in the Late Permian caused by the Gondwanide Orogeny resulted in the reversal of the paleocurrent direction and an influx of felsic volcanic detritus, plagioclase, and quartz from the Gondwana margin (Barrett, 1991; Collinson et al., 1994).

Victoria Group – Triassic

The Fremouw Formation disconformably overlies the Buckley Formation (Barrett, 1991; Collinson et al., 1994). The lower contact of the Fremouw Formation is identified by the change from carbonaceous to noncarbonaceous beds (Collinson et al. 1994). The Fremouw Formation consists of 3 members (Barrett, 1991). The lowest member is fining-upward medium to coarse-grained trough cross-bedded sandstones that has a thickness of about 50 m and is interpreted as an extensive channel system (Barrett, 1991; Collinson et al., 1994). A seasonal equable climate has been suggested for the lowest Fremouw Formation by a diverse fauna of reptiles and amphibians assigned to the *Lystrosaurus* Zone, and therefore of Early Triassic age (Barrett, 1991; Collinson et al., 1994). The middle member has a thickness of about 300 m and consists

of volcanogenic sandstones and mudstones, which are interpreted as flood plain and minor channel deposits (Barrett, 1991; Collinson et al., 1994). The environment of deposition supported a wide variety of well-preserved and complete fossils including not only reptiles and amphibians but also root traces and calamitid stems (Barrett, 1991). The upper member consists of a thick sandstone unit (220-450 m thick) with a quartzose basal unit that is 30 m thick (Collinson et al., 1994). The basal quartzose unit, which contains numerous vertebrate fossils (Collinson et al., 1994) is overlain by sandstone units up to 100 m thick separated by thin silts and mudstones (Collinson et al., 1994). These sandy braided-stream deposits consist primarily of medium to fine sandstones (Collinson et al., 1994). *Dicroidium odontopteroides*, a seedfern that is typical of the Late Triassic, is found throughout the upper member and in the lower Falla Formation (Barrett, 1991; Collinson et al., 1994). The upper 100m of the Fremouw Formation, like the lower Falla Formation, is a coarse grained pebbly sandstone with thin carbonaceous mudstones that are heavily laden with fossilized wood, *in situ* stumps that record fossil forests, and blocks of permineralized peat. The sandstone and mudstone alternation is the consequence of major flooding of braided streams (Barrett, 1991; Collinson et al., 1994).

The overlying Falla Formation, 250m thick, is a cyclic series of coarse grained sandstones with carbonaceous mudstones, which were deposited by low sinuosity rivers flowing to the northwest (Barrett, 1991; Collinson et al., 1994). The occurrence of *Dicroidium odontopteroids* and identification of pollen and spores date the Falla Formation to the late Triassic (Elliot, 1996). The upper contact of the Falla Formation is identified by the abrupt appearance of tuffaceous beds and has been designated as the end of the Victoria Group and the Beacon Supergroup (Elliot, 1996).

Hanson Formation - Jurassic

The Hanson Formation is up to 200 m thick, and consists of tuffs, subordinate tuffaceous sandstones, minor arkosic grits that grade up to sandstone, and minor lapillistones. Tuffaceous beds, which are older than the Ferrar Group, are assigned to the Early Jurassic due to the known age of the underlying formation and the radiometric age of the overlying Kirkpatrick Basalt (Elliot, 1996) and confirmed by vertebrate paleontology (Hammer and Hickerson, 1994). The paleoflow during deposition of the Hanson Formation was in a northwestern direction (Barrett, 1991; Collinson et al., 1994).

III. Ferrar Group

Extrusive Rocks

The Ferrar Group extrusive rocks, which overlie the Hanson Formation, are made up of basaltic pyroclastic deposits and basalt flows. The pyroclastic deposits are identified as the Prebble Formation and range in thickness from 200 m to 400 m thick (Hanson and Elliot, 1996). These pyroclastic deposits consist predominantly of basaltic tuff breccia and lapilli tuff in stratified sequences (Elliot and Fleming, 2008). The pyroclastic deposits show evidence of formation by phreatomagmatic (magma-water interactions) processes (Hanson and Elliot, 1996; Elliot and Fleming, 2008). The predominant pryoclasts in the lapilli-tuffs and tuff-breccias are of vesicular basalt. Dense clasts include dolerite, basalt, sandstone, and occasional silicic tuff and granite, and high proportions of quartz, feldspar, and minor garnet in the matrix (Elliot and Fleming, 2008).

Lava flows, the Kirkpatrick Basalt, crop out in widely separated areas in the central Transantarctic Mountains (Elliot and Fleming, 2008). The extant outcrop in the CTM is

estimated to be approximately 110 km^2. Other outcrop regions have been identified in North Victoria Land and South Victoria Land. The Kirkpatrick Basalt is the uppermost unit in the Gondwana sequence, but its thickness varies greatly as a result of erosion, being absent in most places. Individual flows range from 1 m to as much as 230 m in thickness, with basalt sequences having up to 41 flows and thicknesses up to 750m (Elliot and Fleming, 2008). The thicker individual flows are probably the result of localized topography and ponding (Elliot and Fleming, 2008). The Kirkpatrick Basalt lavas exhibit a wide range of characteristics such as massive coarse-grained intervals, hackly fractured intervals, columnar jointing, and pahoehoe textures (Elliot and Fleming, 2008).

Intrusive Rocks

The Ferrar Group intrusive rocks consist of the Dufek intrusion and the Ferrar Dolerites. The layered mafic Dufek intrusion crops out in two ranges up to 40+ km apart, with an estimated areal extent of 6600 km^2 and a total volume estimated to be $0.6x10^5 km^3$ (Elliot and Fleming, 2008).

The Ferrar Dolerite is a collection of massive bodies, sills, and dikes that vary in thickness up to 700 m thick. The minimum areal extent of a single Ferrar sill is estimated to be 5000 km^2 (Elliot and Fleming, 2004). The sills are predominantly found in the Beacon Supergroup strata, and generally range in thickness between 100 m and 200 m thick, but in the Dry Valleys region sills are up to 700 m thick (Elliot and Fleming, 2004). The sills are the dominant expression of the Ferrar Dolerite. The Ferrar dikes are numerous but volumetrically insignificant compared to the sills (Elliot and Fleming, 2004). The dikes generally range in thickness from 0.2 m to 3 m with sparsely occurring dikes up to 30 m thick, extend only a few

km in outcrop length, and are often segmented. Dike swarms have not been identified, and very few massive feeder dikes have been identified. Possible volcanic or sub-volcanic centers are widely scattered and are 10 – 100 m across in diameter (Elliot and Fleming, 2004).

Age of the Ferrar Group

The Ferrar Group has been dated by the K-Ar, Rb-Sr, $^{40}Ar/^{39}Ar$, and U-Pb techniques. The large range of ages determined by the K-Ar technique is attributed primarily to loss of Ar, a result of mid-Cretaceous alteration of the rocks (Fleming et al., 1995). Using the $^{40}Ar/^{39}Ar$ incremental heating method on plagioclase grains Heimann et al. (1994) determined the age of emplacement of the Ferrar to be 176.6 ± 1.8 Ma. Fleming et al. (1997) used the same method as Heimann et al. (1994) and determined the age of the Ferrar Dolerite to be 176.7 ± 1.8 Ma. The $^{40}Ar/^{39}Ar$ dates showed consistent results that the overall emplacement occurred in less than 1 m.y. for both lavas (Heimann et al., 1994) and sills (Fleming et al., 1997). The application of the U-Pb dating technique using zircon and baddeleyite grains from two dolerite sills, one located in the central Transantarctic Mountains and the other in south Victoria Land, has given an age of 183.6 ± 1.8 Ma (Encarnación et al., 1996). The U-Pb date is regarded as the best estimate of the emplacement age of the Ferrar Group because mid-Cretaceous alteration of the Ferrar rocks resulted in variable Ar concentrations, affecting the K-Ar and $^{40}Ar/^{39}Ar$ ratios (Encarnación et al., 1996; Fleming et al., 1997). The accuracy of $^{40}Ar/^{39}Ar$ is dependent on the age assigned to the standard and to the calibration uncertainties within and between laboratories, resulting in a greater range of uncertainty than that of the U-Pb technique (Encarnación et al., 1996; Fleming et al., 1997). The whole-rock $^{40}Ar/^{39}Ar$ age recalculated by Fleming et al., (1997) and Encarnación et al. (1996), using a slightly older monitor age, determined an age (180.4 ± 1.5 Ma) which is within uncertainty of the mean U-Pb age for the Antarctic sills, 183.6±2.1 Ma.

Currently, single zircon grains are being analyzed with the expectation that the uncertainties will be reduced to ± 0.1-0.2 Ma.

IV. Field Relations

Samples from 12 sills and dikes in the Beardmore Glacier region in the CTM, and 8 sills and dikes from other areas were analyzed (Table 1). The Beardmore Glacier samples were collected by David H. Elliot, the other samples came from the U.S. Polar Rock Repository. Locations of the samples are indicated in Figure 2, and the stratigraphic column (Figure 3) shows the generalized distribution of sills in the Beacon in the Beardmore Glacier region. Most of the samples analyzed are from the chilled margins of sills and dikes.

V. Petrography

In thin section the samples are dominantly composed of plagioclase and pyroxene with variolitic to ophitic textures. The plagioclase forms microphenocrysts in some rocks. Clinopyroxene is identifiable in all samples, but the distinction between augite and pigeonite cannot be determined in most samples due to the small grain size of the pyroxene crystals and secondary alteration. Previous thin section analysis suggests the dominant pyroxene phase present is augite with pigeonite being subordinate. The samples also contain irresolvable interstitial matrix, opaques, and granophyric intergrowths. The irresolvable interstitial matrix is largely unidentifiable due to the fine-grain texture. The occasional occurrence of granophyric intergrowths suggest the presence of plagioclase and quartz. Fe-rich opaques occur mainly as disseminated grains throughout the matrix, but also occur as small phenocrysts.

Table 1. Location of sills and dikes from the Beardmore Glacier region, includes samples collected by Dr. Elliot in the field and other samples provided from Byrd Polar Rock Repository, an NSF facility. Locations on Figures 1 and 2.

Sample	Location	Lat.	Long.	
2-2	W ridge Fremouw Peak	S 84.30	E 164.20	Sill contact
2-3	W ridge Fremouw Peak			Sill contact
2-9	W ridge Fremouw Peak			Dike contact
2-17	Summit of Fremouw Peak			Sill contact
5-3A	E ridge Fremouw Peak	S 84.30	E 164.41	Sill contact
5-3B	E ridge Fremouw Peak			Sill contact
8-7	N end of ridge E of Fremouw Peak	S 84.31	E 164.57	Sill contact
12-6	NW ridge of Fremouw Peak	S 84.29	E 164.34	1 m from contact
20-6	Wahl Glacier region	S 85.01	E 165.55	Sill contact
34-7	E ridge of Mt. Wild	S 84.80	E 162.62	Sill contact
43-2	W of Buttress Peak	S 84.45	E 163.42	2.4 m from contact
94-10	Ford Spur	S 84.85	E 173.61	Dike contact
4785	Mt. Tukotok, Freyberg Mtns	S 72.28	E 164.71	Sill contact
9873	Abele spur, Forrestal Range	S 83.21	W 051.08	Sill
9964	Mt. Spann, Argentina Range	S 82.05	W 041.35	Sill contact
9989	Pecora Escarpment	S 85.63	W 068.70	Sill
10211	Cordiner Peaks, Pensacola Mtns	S 82.80	W 053.50	Dike contact
10228	Mt. Schopf, Ohio Range	S 84.80	W 113.41	Sill
10234	Pecora Escarpment	S 85.63	W 068.70	Sill
12112	Mt. Schopf, Ohio Range	S 84.380	W 113.41	Sill

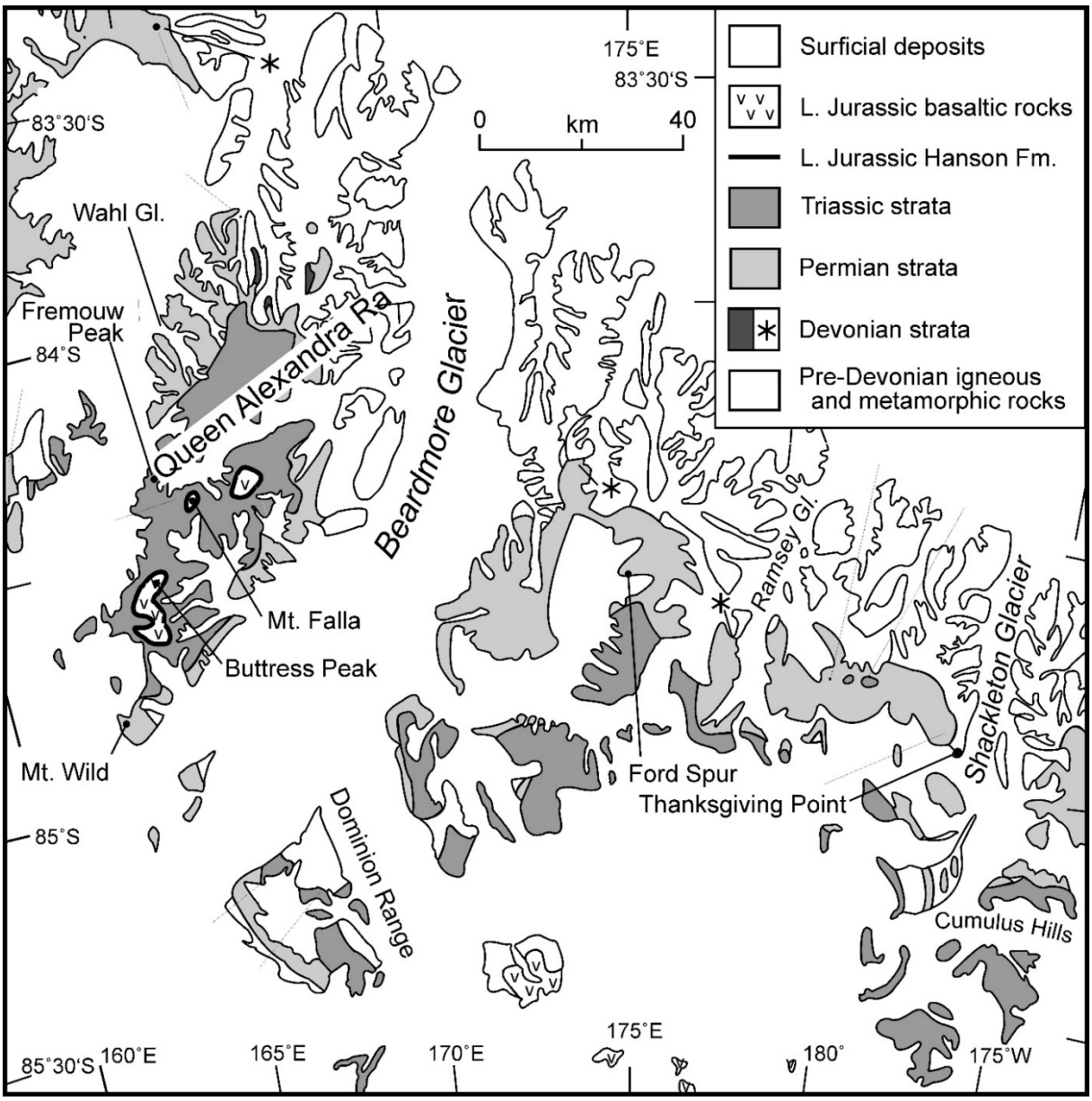

Fig. 2. Location and simplified geologic map for the Beardmore Glacier Region, central Transantarctic Mountains.

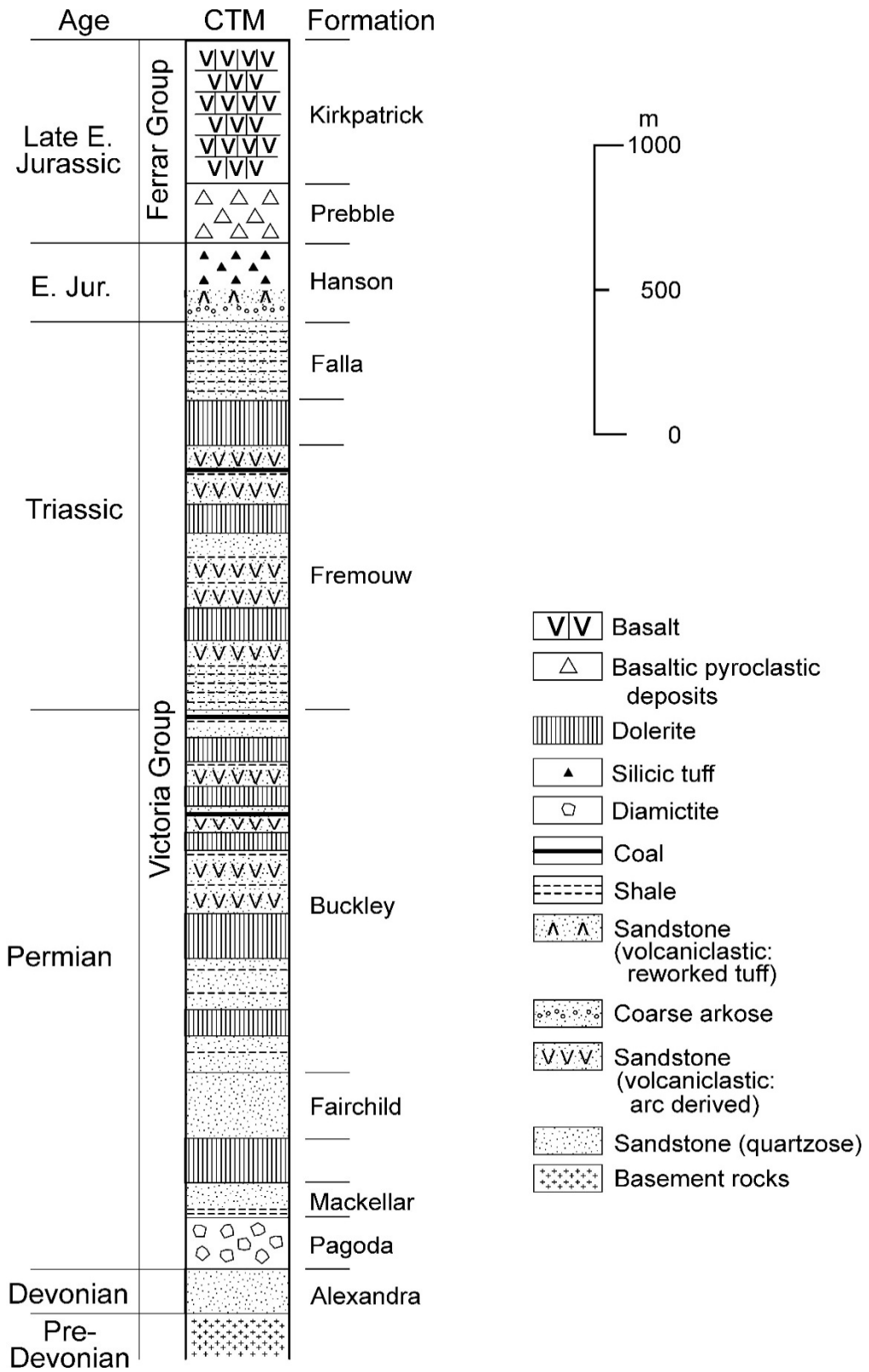

Fig. 3. Diagrammatic and composite stratigraphic column for the Beardmore Glacier region, Antarctica.

Two samples show distinctive secondary mineraloid formation. The samples have undergone slight to moderate alteration. The most prevalent alteration is exhibited by the pyroxene crystals, and occurs as an unidentifiable brown fibrous mineral that could be amphibole. Samples (5-3A, 5-3B) all show the same alteration and, petrographically, are distinctly different from all other samples analyzed. The samples have a quartzo-feldpathic groundmass between elongate plagioclase microphenocrysts, together with aggregates of plagioclase phenocrysts, and a secondary mineraloid, which is the result of secondary alteration.

Sample 9873 differs significantly from all others. The rock is dominated by plagioclase and clinopyroxene, identified as augite, but also includes a significant quantity of orthopyroxene. The sample also has a significant quantity of opaque grains and a small amount of biotite together with minor interstitial quartz. Minor alteration of the orthopyroxene grains is observed as a low interference fibrous alteration which is probably an amphibole. The rock, from the Dufek Intrusion, although described as a basalt or dolerite, is better described as an iron-rich dolerite or gabbro.

VI. Chemistry

Previous Work

Most previous geochemical analyses of the Ferrar group have been focused on samples that represent the extrusive lava flows (Siders and Elliot, 1985; Fleming et al., 1995; Elliot et al., 1999). High initial $^{87}Sr/^{86}Sr$ isotope ratios of dolerites that have been identified in the Ferrar Group are attributed to crustal assimilation rather than representing an unmodified upper mantle composition (Fleming et al., 1995; Fleming et al., 1999). This suggests that the Ferrar rocks were either derived from an enriched mantle source or were the result of crustal assimilation by

mantle derived magmas (Fleming et al., 1999). Two different chemical compositions have been identified for the rocks of the Ferrar Group based on geochemical analysis (Fleming et al., 1995). The SPCT has a limited compositional range which has only been identified in the uppermost lava flows of the Kirkpatrick Basalt (Elliot et al., 1999) and in sills of the Whichaway Nunataks and Theron Mountains. The MFCT has a range of compositions from 8-9% MgO to more evolved rocks with 3-4% MgO (Elliot et al., 1995). The MFCT exhibits abrupt decreases in compatible elements (e.g. Ni, Cr), with steady increase in large-ion lithophile elements (LILE) (e.g. K, Ba) and high-field-strength elements (HFSE) (e.g. Zr, Y, Ce). Only the olivine-bearing dolerite sills of the MFCT fall into the MgO range of 8-9%. The more evolved rocks, consisting of both basalts and dolerites, have an MgO range of 3-7%. The more evolved rocks (MgO < 4.5%) are all lavas, and the less evolved rocks include both sills and lavas. Even the most mafic rocks (MgO > 9%) have isotopic and trace element characteristics that reflect crustal contamination of mantle magma, as demonstrated by Nb and Ta depletion as well as Pb enrichment (Fleming et al., 1995).

New Data

Twenty samples were analyzed for major and trace element abundances (Table 2, Table 3). Major and trace element concentrations were determined using X-Ray Fluorescence, Inductively Coupled Plasma Mass Spectrometry, and Inductively Coupled Plasma Optical Emissions techniques. The samples show a range of compositions from less evolved to more evolved (MgO = 10.3 - 1.3%; Mg number = 69.5 – 24.6). The analyses lie in the MFCT range of compositions. The major oxide and trace element concentrations are plotted against Mg number which is the best indicator of basaltic magma evolution, and reflects fractionation of plagioclase

Table 2. Major Element Analyses by XRF of Ferrar Large Igneous Province samples from the Transantarctic Mountains.

Sample	SiO_2	TiO_2	Al_2O_3	Fe_2O_3	MnO	MgO	CaO	Na_2O	K_2O	P_2O_5
2-2	52.08	0.48	16.01	9.18	0.19	9.18	11.26	1.21	0.35	0.06
2-3	52.25	0.48	16.04	9.26	0.17	8.75	11.29	1.37	0.33	0.06
2-9	52.43	0.49	16.16	9.11	0.16	8.30	11.42	1.50	0.38	0.06
2-17	51.50	0.44	15.71	9.28	0.16	10.33	10.91	1.26	0.33	0.06
5-3A	68.46	0.70	16.95	5.57	0.10	1.28	1.96	1.62	3.29	0.09
5-3B	66.57	0.69	17.98	6.30	0.12	1.51	2.10	1.56	3.10	0.08
8-7	53.46	0.56	15.89	9.51	0.16	7.11	11.03	1.81	0.37	0.09
12-6	53.96	0.61	15.08	9.90	0.18	6.98	9.81	2.30	1.07	0.09
20-6	54.19	0.58	16.13	8.97	0.14	7.09	10.71	1.87	0.21	0.09
34-7	55.58	0.85	14.64	10.84	0.18	5.41	9.11	2.02	1.19	0.14
43-2	52.43	0.58	15.68	9.68	0.17	7.93	10.75	1.90	0.80	0.08
94-10	54.02	0.62	15.02	9.83	0.17	7.22	10.07	2.24	0.74	0.08
4785	53.56	0.61	15.03	9.96	0.17	7.22	10.93	1.83	0.59	0.09
9873	48.35	2.67	12.66	21.20	0.27	3.38	9.22	1.30	0.57	0.38
9964	55.35	0.63	14.86	9.59	0.16	6.35	10.19	1.94	0.83	0.10
9989	54.42	0.75	14.54	10.89	0.18	5.97	10.23	1.96	0.94	0.10
10211	55.60	0.62	14.85	9.48	0.16	6.34	10.20	1.84	0.80	0.10
10228	56.31	1.34	13.25	13.25	0.19	3.57	8.13	2.28	1.48	0.20
10234	55.14	0.82	14.13	11.19	0.18	5.69	9.64	2.06	1.03	0.12
12112	56.35	1.34	13.31	13.16	0.18	3.73	8.39	2.12	1.23	0.18

Table 3. Trace Element Analyses by ICP-MS and ICP-OES of Ferrar Large Igneous Province samples from the Transantarctic Mountains.

Sample	Cr	Rb	Sr	Ba	Y	Zr	Ce	La
2-2	323	11	93	90	14	49	12	6
2-3	312	11	83	76	13	45	11	5
2-9	308	12	106	81	12	46	11	5
2-17	312	9	112	86	11	41	10	5
5-3A	42	111	111	474	25	80	62	29
5-3B	51	103	107	428	24	60	54	25
8-7	180	12	90	93	15	106	16	8
12-6	104	28	154	253	17	66	17	8
20-6	188	5	118	56	15	48	16	7
34-7	83	30	92	209	22	100	29	13
43-2	206	25	137	149	16	64	17	8
94-10	111	22	173	268	18	67	18	8
4785	141	19	100	162	20	34	23	10
9873	5	20	165	240	55	82	41	18
9964	138	28	127	207	21	99	25	12
9989	51	37	114	229	26	115	29	13
10211	144	28	137	234	22	101	26	12
10228	17	63	124	358	40	137	48	21
10234	62	42	125	259	29	129	33	15
12112	17	47	141	368	40	169	48	22

and pyroxene. Major elements SiO_2, TiO_2, FeO, Na_2O, K_2O, and P_2O_5 show a positive correlation with Mg number (Fig. 4) whereas CaO and Al_2O_3 exhibit a negative correlation with Mg number (Fig. 4). The trends displayed by the major elements are representative of early crystallization of Ca-rich plagioclase and pyroxene from a fractionating melt. Trace elements Rb, Ba, Y, Zr, Ce, and La all increase as the magma evolves (Fig. 5). Zr, Ce, La, and Y are high field strength elements and strongly incompatible, therefore the abundances increase as the melt evolves by fractionation. Rb and Ba are large-ion lithophile (LIL) elements which can substitute for K in the late stage crystallization of an evolving magma. Secondary alteration may account for the scatter that is exhibited by Ba (Fig. 5), Pb (not illustrated) and K. Cr decreases with magma evolution, which is expected because Cr substitutes in clinopyroxene. Sr, a mobile element, exhibits scatter but there is no distinguishable trend of change during fractionation. The Sr scatter in Ferrar rocks has been attributed to hydrothermal/low temperature alteration during the Cretaceous (Fleming et al., 1995). The major and trace element trends of the majority of the analyzed samples are typical of a magma evolving by fractional crystallization.

Two samples are anomalous with respect to the trends of fractional crystallization. Samples 5-3A and 5-3B are characterized by low Mg-numbers (32.0 and 32.9), high SiO_2, Al_2O_3, and K_2O, and low TiO_2, Fe_2O_3, P_2O_5, MgO, MnO, CaO, Y. The mobile LIL elements (Ba and Rb) are very high and two of the high field strength incompatible elements (Y and Zr) are very low. The geochemistry suggests considerable secondary alteration with both addition and leaching of elements

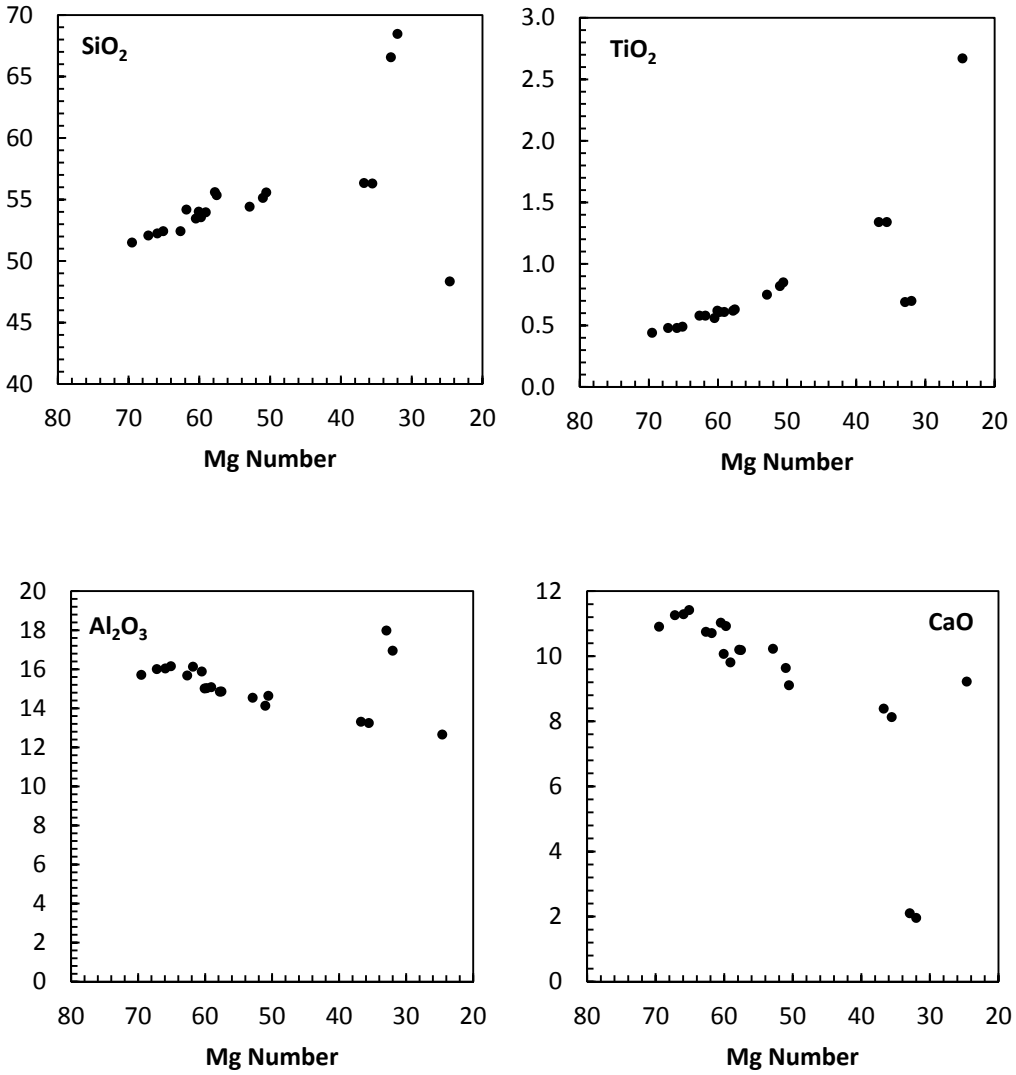

Fig. 4. Chemical variation diagrams for major elements (weights in oxide-percent) against Mg-number (Mg/(Mg+Fe^{2+}) for analyzed samples. Chemical analyses of the rocks dated in this study are given in Table 1. Mg-number decreases with increasing magma evolution (Fleming et al., 1997)

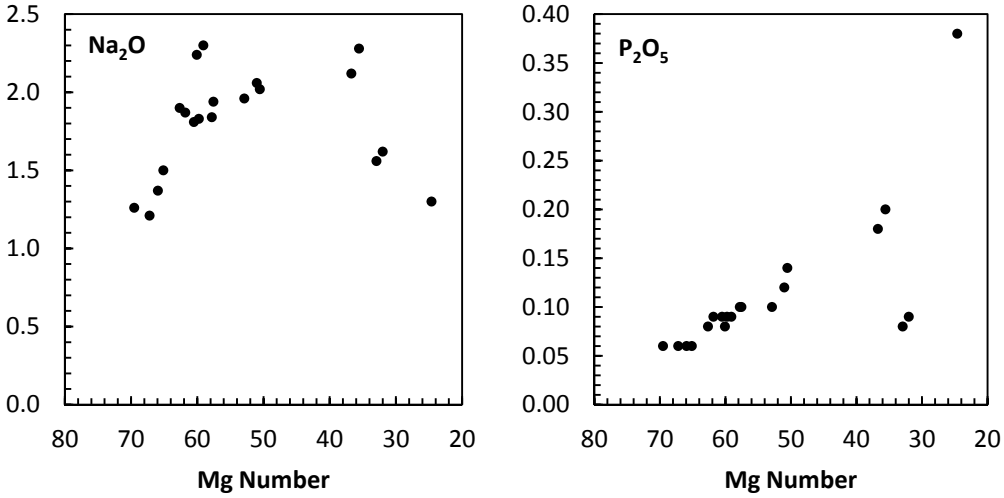

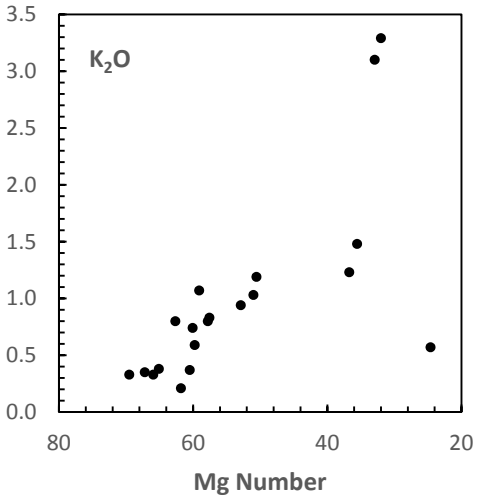

Fig. 4. (continued)

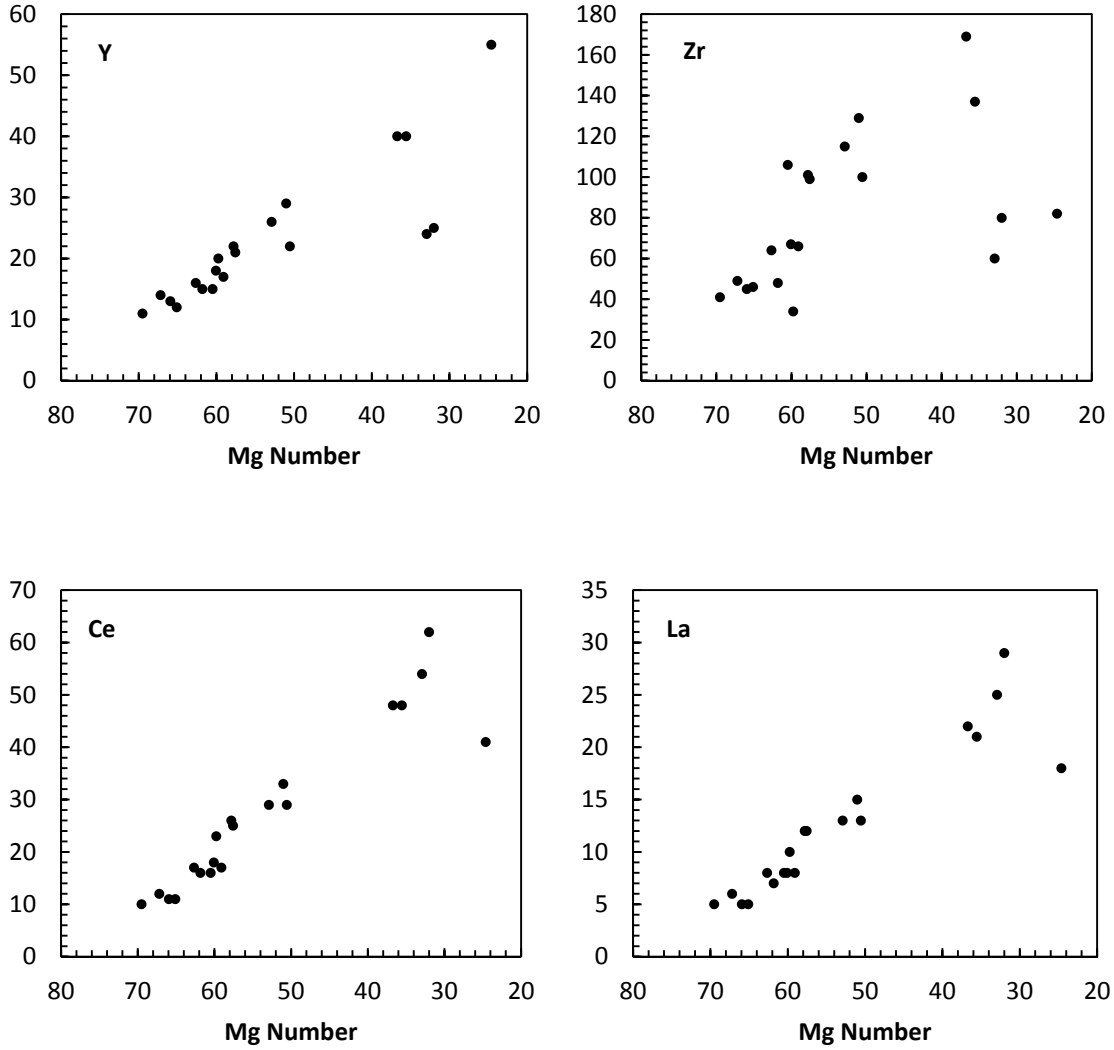

Fig. 5. Variation diagrams for selected trace elements (in ppm) against Mg-number (Mg/(Mg+Fe^{2+}) for analyzed samples.

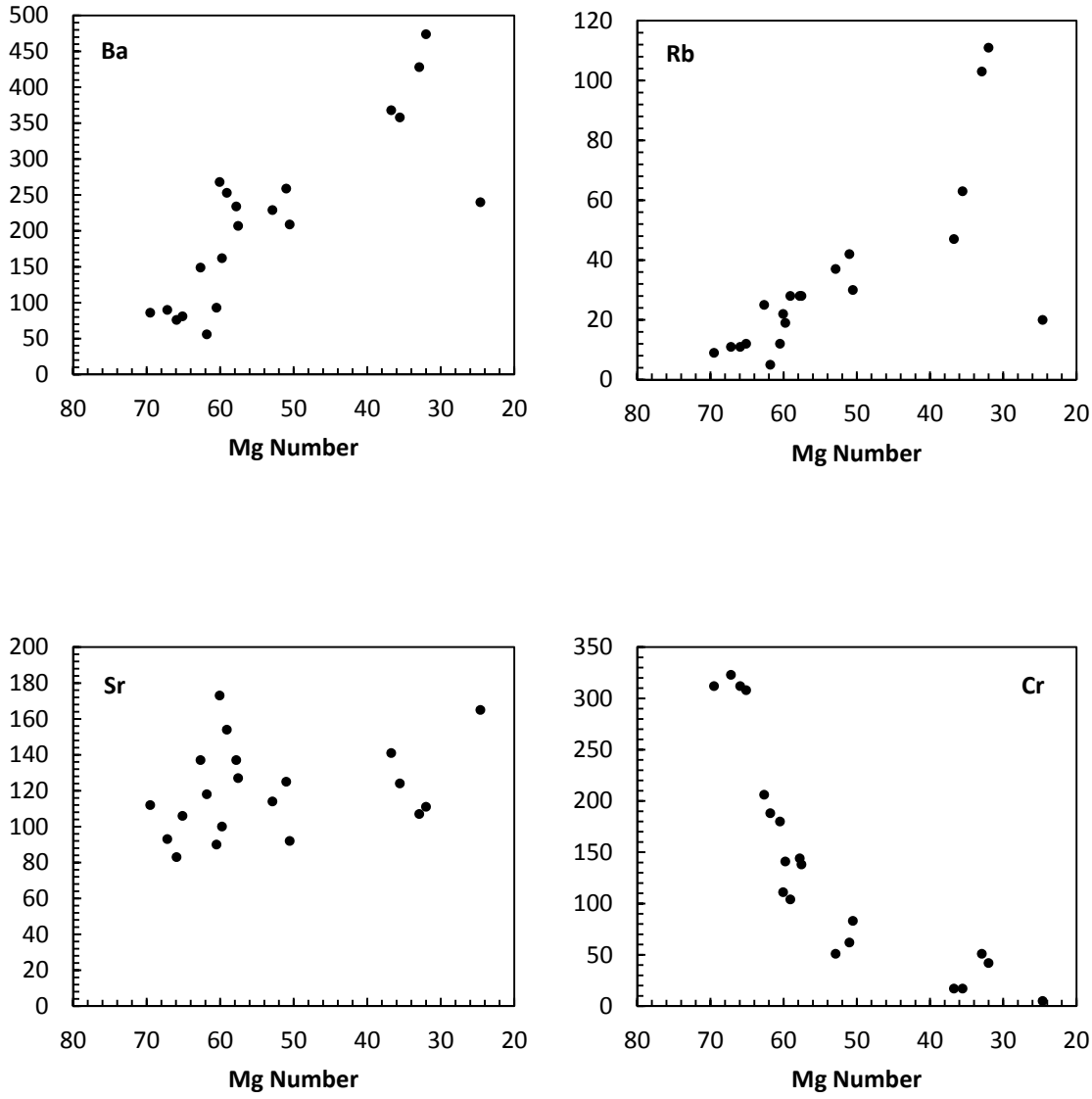

Fig. 5 (continued)

Discussion

The new data for sills of the Ferrar Dolerite correlate with previous results. None of the samples falls within the geochemical values of the SPCT. The majority of the samples exhibit the same major and trace element trends and also have similar abundances and depletions or enhancements in Nb, Ta, and Pb as occur in MFCT rocks. The chemical concentrations of these samples suggest the rocks were crystallized from the MFCT magma type, and exhibit different stages of fractional crystallization. Three samples are easily identified as different with respect to the geochemical trends. Two samples exhibit strong secondary alteration and the third sample is an iron-rich dolerite or gabbro.

Four samples (2-2, 2-3, 2-9, and 2-17) have the highest MgO (>8%) of all the dolerite samples. The presence of olivine, observed as psuedomorphs in thin section, accounts for the abundance of MgO and distinguishes these samples as olivine dolerites. The presence of olivine makes these four samples the least evolved of the samples analyzed and are slightly less evolved geochemically than the other dolerites analyzed.

The most obvious distinction of samples 5-3A and 5-3B is the secondary alteration and the mineralogy which is dominated by feldspar laths and a quenched quartzo-feldspathic matrix. These two samples have greater abundances of SiO_2, Al_2O_3, Ba, and Rb. TiO_2, CaO, Na_2O, P_2O_5, Y, Zr, are less abundant in these two samples than in the others. The different abundances and depletions of major and trace elements is attributed to the rock's evolved composition and strong alteration to a mineraloid. The two samples contain an abundance of SiO_2, Al_2O_3, and K_2O which reflects the abundant feldspar and quartzo-feldspathic matrix. The low MgO is

consistent with the apparent absence of unaltered pyroxene, and the opaques must account for much of the iron.

Sample 9873 was collected from Abele Spur within the Forrestal Range, within what was visually identified as a basalt or dolerite body. In thin section, sample 9873 consists of plagioclase, augite, orthopyroxene, opaques, and minor biotite and apatite. It does not follow the trends exhibited by the other samples and has a distinctive low Mg-number. Many of its element abundances are outliers in comparison with the other samples. The mineralogy and geochemical analysis are typical of tholeiitic magmas that evolve to strong Fe-enrichment, as is seen in layered basic intrusions and is consistent with it being part of the Dufek intrusion.

The low SiO_2 and MgO is the result of early crystallization of Mg-rich pyroxenes, which leads to Fe-enrichment and associated increase in TiO_2 and incompatible elements. This is reflected in the abundant opaques, which contain the TiO_2, and the minor biotite. The LIL elements are probably substituting for K in biotite, and the LILEs are probably present in apatite.

The new data for the CTM sills correlate with previously collected data for the Ferrar dolerites. The sills exhibit the same major and trace element chemical signature as the MFCT lavas. The similar compositions indicates that the new sill samples share the same source as for the previously analyzed sills and lavas. The analyses also suggest that the rocks evolved by similar processes of fractional crystallization. None of the sills analyzed exhibit the SPCT composition. The samples analyzed all have MFCT composition, which supports the notion that the Ferrar magmas were derived from a single source (Fleming et. al., 1997). The Ferrar, emplaced over a distance of 3000 km, is unique compared to other flood basalts because of the

single magma source and the dominance (99%) of a single magma type; other flood basalts are composed of multiple magma types derived from several sources.

Conclusion and Suggestions for Future Work

The chemistry of the samples from the Transantarctic Mountains all fall into the classification of the MFCT composition type of the Ferrar Large Igneous Province. Three samples are outliers amongst the data, two have been strongly altered, possibly in the mid-Cretaceous, and the third rock has a highly evolved Fe-rich composition and mineralogy, which indicates it is part of the Dufek Layered basic intrusion. The similarity among the chemical compositions of these MFCT rocks provides substantial evidence that they were formed by the same processes as other previously analyzed MFCT sills and lavas. Their chemistry also indicates evolution by the process of fractional crystallization dominated by pyroxene and plagioclase. These samples further demonstrate the continuity of the Ferrar Group over a linear extent exceeding 3000 km. This is a unique attribute of the Ferrar Large Igneous Province compared to other large igneous provinces. This research adds to the present geochemical database for the Ferrar Group. Further investigations by expanding the geographic coverage of chemical data, and age dating of samples collected, will contribute to a better understanding of the space-time-geochemical relationships and the mode of transport for the Ferrar Large Igneous Province.

References

Barrett, P.J. 1991. The Devonian to Jurassic Beacon Supergroup of the Transantarctic Mountains, *in* Tingey, R.J., ed., The Geology of Antarctica, New York: Oxford University Press, 120-147.

Burgess, S.D., Fleming, T.H., Elliot, D.H., and Bowring, S.A. 2011. High-precision U-Pb zircon geochronology of the Ferrar large Igneous Province: Can sill emplacement be linked with the Pliensbachian-Toarcian extinction event? *Geological Society of America*, Abstracts with Programs, v. 43, p. 372.

Collinson, J.W., Isbell, J.L., Elliot, D.H., Miller, M.F., Miller J.M.G. 1994. Permian – Triassic Transantarctic Basin, *in* Veevers, J.J. and Powell, C. McA., eds., Permian Triassic Pangean Basins and Foldbelts Along the Panthalassan Margin of Gondwanaland, Boulder, CO, *Geologic Society of America Memoir 184,* p. 173-222.

Elliot, D.H., Fleming, T.H., Haban, M.A., Siders, M.A. 1995. Petrology and mineralogy of the Kirkpatrick Basalt and Ferrar Dolerite, Mesa Range region, north Victoria land, Antarctica, *in* Elliot, D.H., and Blaisdell, G.L., eds., Contributions to Antarctic Research IV: American Geophysical Union, *Antarctic Research Series*, v. 67, p. 103-142.

Elliot, D.H. 1996. The Hanson Formation: a new stratigraphical unit in the Transantarctic Mountains, Antarctica. *Antarctic Science*, v. 8, p. 389-394.

Elliot, D.H., Fleming, T.H., Kyle, P.R., Foland, K.A. 1999. Long-distance transport of magmas in the Jurassic Ferrar Large Igneous Province, Antarctica. *Earth and Planetary Science Letters*, v. 16, p. 89-104.

Elliot, D.H., Fleming, T.H. 2004. Occurrence and Dispersal of Magmas in the Jurassic Ferrar Large Igneous Province, Antarctica. *Gondwana Research,* v. 7, p. 223-237.

Elliot, D.H., Fleming, T.H. 2008. Physical volcanology and geological relationships of the Jurassic Ferrar Large igneous Province, Antarctica. *Journal of Volcanology and Geothermal Research,* v. 172, p. 20-37

Encarnación, J., Fleming, T.H., Elliot, D.H., Eales, H.V. 1996. Synchronous emplacement of Ferrar and Karoo dolerites and the early breakup of Gondwana. *Geology*, v. 24, p. 535-538.

Fleming, T.H., Foland, K.A., Elliot, D.H. 1995. Isotopic and chemical constraints on the crustal evolution and source signature of Ferrar magmas, north Victoria Land, Antarctica. *Contributions to Mineral Petrology*, v. 121, p. 217-236.

Fleming, T.H., Heimann, A., Foland, K.A., Elliot, D.H. 1997. $^{40}Ar/^{39}Ar$ geochronology of Ferrar Dolerite sills form the Transantarctic Mountains, Antarctica: Implications for the age and origin of the Ferrar magmatic province. *Geological Society of America Bulletin,* v. 109, p. 533-546.

Fleming, T.H., Foland, K.A., Elliot, D.H. 1999. Apophyllite $^{40}Ar/^{39}Ar$ and Rb-Sr geochronology: Potential utility and application to the timing of secondary mineralization of the Kirkpatrick Basalt, Antarctica. *Journal of Geophysical Research*, v. 104, p. 20081 – 20095.

Goodge, J.W., Fanning, C.M. 2002. Precambrian history of the Nimrod Group, central Transantarctic Mountains, Gamble, J.A., Skinner D.N.B., Henrys, S. (*eds.*), Antarctica at the Close of a Millenium. *Royal Society of New Zealand Bulletin*, v. 35. p. 43-50.

Hammer, W.R., Hickerson, W.J. 1994. A new crested theropod dinosaur from Antarctica. *Science*, v. 264, p. 828-830.

Hanson, R.E., Elliot, D.H. 1996. Rift-related Jurassic basaltic phreatomagmatic volcanism in the central Transantarctic Mountains: precursory stage to flood-basalt effusion. *Bulletin of Volcanology*, v. 58, p. 327-347.

Heimann, A., Fleming, T.H., Elliot, D.H., Foland, K.A. 1994. A short interval of Jurassic continental flood basalt volcanism in Antarctica as demonstrated by $^{40}Ar/^{39}Ar$ geochronology. *Earth and Planetary Science Letters*, v. 121, p. 19-41.

Isbell, J.L. 1999. The Kukri Erosion Surface; a reassessment of its relationship to the rocks of the Beacon Supergroup in the central Transantarctic Mountains, Antarctica. *Antarctic Science*, v. 11, p. 228-238.

Siders, M.A., Elliot, D.H., 1985. Major and trace element geochemistry of the Kirkpatrick Basalt, Mesa Range, Antarctica. *Earth and Planetary Science Letters,* v. 72, p. 54-64.

Stump, E. 1995. *The Ross Orogen of the Transantarctic Mountains*. Melbourne: Cambridge University Press, 304 pp.

Appendix

Petrographic descriptions

2-2 Fremouw Peak. Fine-grained dolerite. Porphyritic with sparse microphenocrysts in a matrix with variolitic texture. Phenocrysts consist of sparse anhedral to euhedral olivine psuedomorphs up to 1.00 mm; olivine replaced by fibrous secondary minerals. Plagioclase, An_{52}, forms subhedral to euhedral laths showing Albite twins, up to 1.2 mm in length. The clinopyroxene is anhedral to subhedral and up to 0.15 mm in length and exhibits some alterations. Sparse anhedral opaques present and are less than 0.1 mm across.

2-9 Fremouw Peak. Fine-grained dolerite. Porphyritic with sparse microphenocrysts in a matrix with variolitic texture. Scattered subhedral olivine pseudomorph phenocrysts are present and up to 0.1 mm in length; replaced by fibrous secondary minerals. Plagioclase, with Albite twinning and composition of An_{54}, forms subhedral to euhedral laths up to 1.0 mm in length. The pyroxene, both augite and pigeonite, is subhedral to anhedral, up to 0.25 mm across, and exhibits minor alteration. Minor interstitial quench crystallization with secondary alteration.

5-3A, B Fremouw Peak. Dolerite. Plagioclase forms elongate crystals in a variolitic texture, and aggregates of smaller crystals, all separated by abundant very fine grained quartzo-feldspathic quench intergrowths. Aggregates of euhedral to subhedral plagioclase phenocrysts with Albite twinning and composition is An_{52} up to 0.75 mm in length. Secondary orange-brown phyllosilicate, an alteration product of glass. Iron-rich opaques, 0.1mm across) disseminated throughout. Groundmass between elongate plagioclase consists of quartzo-feldspathic intergrowths and secondary phyllosilicates.

8-7 Fremouw Peak. Fine-grained dolerite. Microphenocrysts of plagioclase are set in fine grained matrix of plagioclase and pyroxene in diabasic texture. Microphenocrysts of plagioclase and clinopyroxene in dispersed aggregates. Plagioclase forms euhedral to subhedral laths less than 0.1 mm in length; Albite twinning and composition of An_{68}. Clinopyroxene is subhedral to euhedral and up to 0.1 mm across. Opaques subhedral to anhedral, maximum dimension 0.01 mm.

12-6 Fremouw Peak. Dolerite. Plagioclase and clinopyroxene occur in a subophitic texture. Plagioclase form euhedral to subhedral laths up to 0.2mm in length, exhibiting Albite twinning with a composition of Ab_{46}. Clinopyroxene anhedral, fine grained up to 0.2 mm in length. Clinopyroxene altered to brown-green phyllosilicate. Sparse subhedral opaques, up to 0.1 mm across.

20-6 Wahl Glacier region. Dolerite. Porphyritic with sparse microphenocrysts in a matrix with variolitic texture. Sparse phenocrysts consist of orthopyroxene, up to 0.5 mm, completely replaced by secondary fibrous minerals. Plagioclase, Ab_{48}, form subhedral to anhedral laths up to 0.5 mm in length. Plagioclase exhibit curving laths, indicative of rapid cooling. Clinopyroxene up to 0.5 mm in length, but mainly as radiating, sheaf-like intergrowths. Disseminated opaques throughout the matrix, less than 0.01mm.

34-7 Mount Wild. Fine-grained dolerite. Porphyritic with sparse microphenocrysts in a matrix with variolitic texture. Sparse phenocrysts of plagioclase with a composition of Ab_{53} (up to 0.5 mm) and clinopyroxene, both augite and pigeonite, up to 0.5 mm. Plagioclase forms subhedral to anhedral laths up to 0.2 mm in length, Albite twinning. Clinopyroxene in radiating, sheaf-like aggregates, subhedral to anhedral and up to 0.1 mm in length. Subhedral to anhedral opaques disseminated throughout sample, under 0.02 mm across.

43-2 Buttress Peak. Dolerite. Plagioclase and clinopyroxene occur in an ophitic texture. Plagioclase, Ab_{43} forms subhedral to anhedral laths up to 1.0 mm in length. Clinopyroxene subhedral to anhedral, up to 1.0 mm in length, includes both augite and pigeonite phases. Iron-rich interstitial patches up to 0.5 mm across. Anhedral opaques, under 0.1 mm in diameter in matrix. Matrix is quenched and altered glass.

94-10 Ford Spur. Dolerite. Plagioclase and clinopyroxene occur in an ophitic texture. Plagioclase, Ab_{46}, forms subhedral to anhedral laths up to 0.5 mm in length. Clinopyroxene forms subhedral to anhedral grains up to 0.5 mm in length; includes both augite and pigeonite. Subhedral to anhedral opaques disseminated throughout sample, under 0.2 mm across. Iron-rich interstitial irresolvable matrix in patches up to 0.3 mm in diameter.

4785 Mount Tukotok. Fine-grained dolerite. Porphyritic with scattered phenocrysts up to 0.6 mm in a very fine grained matrix with intergranular texture. Clinopyroxene microphenocrysts as subhedral to anhedral crystals up to 0.1 mm in length, and as aggregates. Plagioclase (An_{50}) forms subhedral to anhedral laths up to 0.2 mm in length. Sparse very fine grained opaques throughout.

9873 Abele Spur. Gabbro. Plagioclase, clinopyroxene, and orthopyroxene occur in an ophitic texture. An_{56} plagioclase forms subhedral to anhedral laths up to 0.5mm in length. Clinopyroxene, augite, forms subhedral to anhedral laths up to 0.5 mm in length. Orthopyroxene forms subhedral to euhedral laths up to 0.5 mm in length, and has a brown fibrous alteration. Subhedral to anhedral biotite sheets up to 0.2 mm in diameter are dispersed throughout the sample. Subhedral to anhedral opaques up to 0.1 mm across. Quartz disseminated throughout sample, up to 1.0 mm across. Apatite needles dispersed.

9964 Mount Spann. Fine-grained dolerite. Porphyritic with scattered microphenocrysts up to 0.3 mm in a very fine grained matrix with an intergranular texture. Aggregates of microphenocrysts of plagioclase (Ab_{49}) and clinopyroxene. Groundmass of plagioclase laths, up to 0.15 mm, and clinopyroxene grains. Trace of opaque grains (less than 0.05 mm), and irresolvable interstitial material.

9989 Pecora Escarpment. Dolerite. Plagioclase and clinopyroxene occur in a subophitic texture. Plagioclase forms euhedral to subhedral laths up to 1.0 mm in length. Plagioclase exhibits Albite twinning and has a composition of Ab_{46}. Clinopyroxene subhedral to euhedral up to 1.0 mm in length, both augite and pigeonite present. Interstitial matrix consists of quartzo-feldspathic intergrowths with scattered opaque grains (<0.1 mm).

10211 Cordiner Peaks. Fine-grained dolerite. Porphyritic with scattered microphenocrysts up to 0.5 mm in a fine grain matrix with an intergranular texture. Plagioclase phenocrysts form euhedral to subhedral laths, composition Ab_{45}. Matrix consists of plagioclase laths (up to 0.1 mm) and clinopyroxene grains, together with irresolvable opaque-rich interstices.

10228 Mount Schopf. Dolerite. Sparse plagioclase and clinopyroxene in a very fine-grained holocrystalline matrix. Plagioclase forms subhedral laths, less than 0.1 mm in length and composition of An_{72}. Clinopyroxene forms subhedral to anhedral grains up to 0.2 mm, and exhibits alteration to a brown-orange phyllosilicate. Matrix is very fine grained, comprises plagioclase laths, pyroxene grains, finely disseminated opaques, and irresolvable material in interstices.

10234 Pecora Escarpment. Dolerite. Plagioclase and clinopyroxene in an ophitic texture. Plagioclase (Ab_{43}) in subhedral laths up to 1.8 mm in length. Pyroxene forms subhedral to anhedral grains up to 1.2 mm in length; both augite and pigeonite present. Granophyric intergrowths of plagioclase and quartz fill interstices. Opaques up to 0.5 mm across, in single crystals and aggregates, mainly in interstitial areas.

12112 Mount Schopf. Dolerite. Elongate (up to 4.0 mm) clinopyroxene and plagioclase crystals in a coarse matrix with an intergranular texture. Plagioclase composition (Ab_{57}) in elongate prisms and matrix grains (<1.0 mm); some secondary phyllosilicate alteration. Clinopyroxene strongly altered to a fibrous mineral. Interstices filled by quartzo-feldspathic intergrowths, some of which are granophyric. Widely distributed opaques (<0.05 mm). Elongate crystals suggest a water-rich environment of crystallization.